

Bamboo: Building Mega-Scale Vision Dataset Continually with Human-Machine Synergy

Yuanhan Zhang, Qinghong Sun, Yichun Zhou, Zexin He,
Zhenfei Yin, Kun Wang, Lu Sheng, Yu Qiao, Jing Shao, Ziwei Liu

Abstract—Large-scale datasets play a vital role in computer vision. But current datasets are annotated blindly without differentiation to samples, making the data collection inefficient and unscalable. The open question is how to build a mega-scale dataset actively. Although advanced active learning algorithms might be the answer, we experimentally found that they are lame in the realistic annotation scenario where out-of-distribution data is extensive. This work thus proposes a novel active learning framework for realistic dataset annotation. Equipped with this framework, we build a high-quality vision dataset—**Bamboo**, which consists of 69M image classification annotations with 119K categories and 28M object bounding box annotations with 809 categories. We organize these categories by a hierarchical taxonomy integrated from several knowledge bases. The classification annotations are four times larger than ImageNet22K, and that of detection is three times larger than Object365. Compared to ImageNet22K and Objects365, models pre-trained on Bamboo achieve superior performance among various downstream tasks (6.2% gains on classification and 2.1% gains on detection). We believe our active learning framework and Bamboo are essential for future work. Code and dataset are available at <https://github.com/ZhangYuanhan-AI/Bamboo>.

Index Terms—Vision Dataset, Human-Machine Synergy.



1 INTRODUCTION

LARGE-scale pre-trained models, either trained in a supervised [27], [37], [71] or unsupervised [10], [14], [29] manner, have become a foundation for modern computer vision. Pre-trained models [53] bring various applications by transferring to downstream tasks. Most importantly, the fuel of this foundation models [6] relies on the availability of increasingly large and diverse datasets [18], [40], [44], [60].

Building a high-quality dataset requires careful consideration in selecting data. However, public datasets are annotated blindly with no differentiation to samples, which brings a colossal waste of annotation budget: Citovsky *et al* [17] indicates that only 70% data in OpenImages [41] can achieve on-par performance to its complete set. Though active learning (AL) researchers extensively study how to select the most valuable samples—informative and in-distribution—from unlabeled data pool [26], [28], [33], [34], [58], [61], [64], [66], [75], we experimentally observe that the current advanced active learning methods, *e.g.* Cluster-Margin [17], Margin [54] and CoreSet [57], are lame in the realistic annotation scenario. Specifically, AL methods select high-informative data at the expense of choosing out-of-distribution data discarded by annotators and not used for model supervised learning. Random sampling selects less high-informative data than AL but includes much more in-

distribution data than AL. As the performance gain bought by data quantity is superior to data quality when annotated data of AL is 70% less than that of random sampling (as shown in Fig. 6), AL is inferior to random sampling for improving model performance. Given this shortage, we propose a novel active learning framework, which cleans off the out-of-distribution data in the unlabeled data pool before active sampling, ensuring the sampled data under active learning is informative and meanwhile in-distribution. This novel framework achieves better than random sampling for boosting supervised learning model performance.

We aim to annotate a mega-scale classification and object detection dataset with our proposed active learning framework. First, we build a comprehensive label system for querying diverse data covering numerous semantics. Specifically, we form a unified label system with a hierarchical structure consisting of 304,048 categories. It integrates label systems from 19 latest public image classification datasets and five object detection datasets and also absorbs 170,586 new categories from knowledge bases, *e.g.* Wikidata [67]. Then, we contribute **Bamboo Dataset**, a mega-scale and information-dense dataset for the pre-training of both classification and detection, which is active annotating by human-machine synergy. Bamboo has three appealing properties:

- **Yuanhan Zhang and Ziwei Liu are with the S-Lab, Nanyang Technological University**
E-mail: {yuanhan002, ziwei.liu}@ntu.edu.sg
- **Qinghong Sun, Zhenfei Yin, Kun Wang and Jing Shao are with SenseTime Research.** E-mail: {sunqinghong, yinzhenfei, wangkun, shaojing}@senseauto.com
- **Yichun Zhou, Zexin He, Lu Sheng are with Beihang University.** E-mail: {buaazyc, jacquesdeh, lsheng}@buaa.edu.cn
- **Yu Qiao is with Shanghai AI Laboratory.** E-mail: qiaoyu@pjlab.org.cn
- **Comprehensive.** It consists of 69M image classification annotations and 28M object bounding box annotations, spanning over 119K visual categories. The scale of the label system and the annotated data are the largest among all the publicly available datasets. We illustrate the comparison of Bamboo and publicly available datasets in the Fig. 1(c).
- **Information-Dense.** We guarantee Bamboo is highly in-

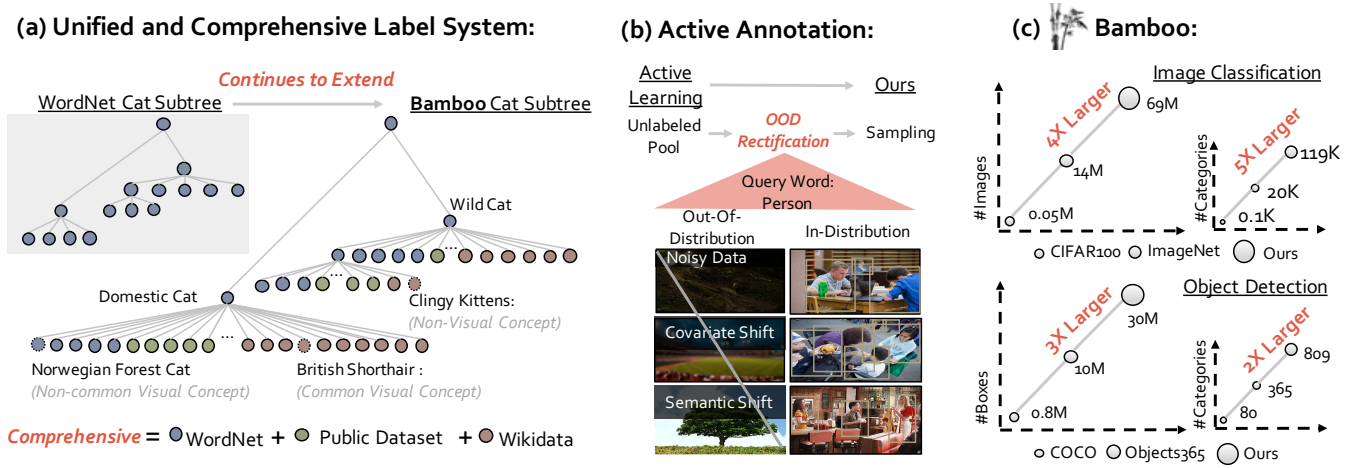


Fig. 1. **The overview of Bamboo Dataset.** Bamboo is a new mega-scale vision dataset built on a comprehensive label system with human-machine synergy. (a) Our label system continually extends from WordNet with our solutions. Concepts in the label system are distinguished as “common visual”, “non-common visual” or “non-visual” concepts. (b) Raw data crawled by the query word *person* includes both the in-distribution (ID) data and out-of-distribution (OOD) data. OOD data implies noisy, covariate shift, and semantic shift data. Noisy data does not present useful semantic information. Covariate shift data implies semantic information, *i.e.* person. However, such semantic information is of poor quality, annotators thus hard to annotate. Semantic shift data also implies semantic information, *i.e.* tree. But the tree is not related to the query word *person*. *OOD rectification* mitigates the ineffectiveness of active learning through filtering OOD data. (c) Bamboo collects 69M classification annotation and 28M bounding box annotations.

formative through the label system and the annotated data. The label system is constructed by thoroughly integrating public datasets and knowledge bases. Our active annotation pipeline specifically selects the annotated data to reduce model uncertainty.

- **Continual.** Our label system keeps the dataset growing with the automatic concept linking strategies. We can constantly absorb new categories in the real world and integrate them into our label system. Moreover, leveraging the ever-increasing internet data, our active annotation pipeline will steadily sustainably expand the Bamboo dataset size.

Extensive experiments demonstrate that Bamboo dataset is an effective pre-training source. The Bamboo pre-trained model significantly outperforms CLIP ViT B/16 [53] pre-trained model with 6.2% gain (85.6% vs 91.8%) on classification, and outperforms Objects365 [59] pre-trained model with 2.1% gain (14.7% vs 12.6%) on CityPersons [79]. In addition, we provide valuable observations regarding large-scale pre-training from over 1,000 experiments. We hope the Bamboo dataset and these observations will pave the way for developing more general and effective vision models.

2 RELATED WORKS

Learning of Representation at Scale. Representation learning has advanced thanks to improvements in various learning paradigms and large-scale datasets. Supervised learning models [15], [30] leverage label information to supervise representation learning, achieving excellent performance among various downstream tasks. To avoid the need for annotations that require a tremendous amount of human and labeling cost, weakly-supervised and self-supervised pre-training methods have been proposed. Self-supervised methods [9], [10], [13], [19], [29], [42], [43], [49], [68], [78] with contrastive learning have shown that unsupervised

pre-training produces features surpassing the supervised feature representations on many downstream tasks [39], [40], [50], [51], [69]. Large weakly-supervised datasets, such as Instagram hashtags [46] and JFT [60], helps model [70], [71], [81] achieve significant gains on downstream tasks. In addition, CLIP [53] pre-train models on both the image signal and text signal, achieving good performance for the zero-shot evaluation. Our study is part of a larger body of work on training models on sizeable supervised image datasets. As the labeling cost that hurdles the supervised learning dataset is becoming increasingly significant, we systematically investigate how to collect, annotate and build a mega-scale dataset efficiently, actively and continually.

Active Learning. Active learning (AL) aims at finding the minimum number of labeled images to have a supervised learning algorithm reach a certain performance [26], [28], [33], [34], [58], [61], [64], [66], [75]. The main component in an active learning loop is sampling strategies. The existing AL research is conducted on the curated datasets. Each data point in the labeled and unlabeled pool of these datasets is valid, *i.e.* available for labeling. However, curated datasets can hardly imitate the annotation in realistic scenarios where out-of-distribution data that is unavailable for labeling appears on a large scale in the unlabeled pool. From our experiments, we find the existing AL methods lag in realistic scenarios. Therefore, we propose a novel active annotation pipeline to improve the performance of AL methods in realistic scenarios.

3 LABEL SYSTEM CONSTRUCTION

In this section, we briefly introduce how to build a comprehensive label system. The number of concepts decides the data amount upper bound—we crawl data based on querying these labels. Starting from WordNet [48], we enrich its concepts from another two concept resources (Sec. 3.1) through three designed linking strategies (Sec. 3.2)).

Visual vs Non-visual Samples



Fig. 2. **The illustration of visual and Non-visual concept.** *Vitamin* do not share any common semantic information. *Economists* implies common semantic information—Man—but economists are not necessarily men.

3.1 Concepts Resources

WordNet. WordNet is a lexical database of semantic relations between concepts in more than 200 languages. Each meaningful concept in WordNet, possibly described by multiple words or phrases, is called a “synset”. Referring to ImageNet22K [18], we only use the Noun words of WordNet. WordNet is the foundation of our label system.

Public Datasets. We collect 24 public datasets, including ImageNet22K [18], OpenImages [41], COCO [44], iNaturalist [65], and *etc.*¹ These datasets cover a wide range of datasets in both image classification and object detection.

Wikidata. Wikidata [67] contains a large number of concepts, such as different kinds of foods, animals, and locations. As the number of concepts in Wikidata continues to grow, so far, we have included 170,586 concepts from it. These concepts are the leaf nodes in their taxonomy.

3.2 Concepts Integration

WordNet is a lexical graph whose concepts imply semantic relation. For example, the father node of “British Shorthair” is “Domestic Cat”. How to integrate concepts from public datasets and Wikidata into this WordNet is an open question. We propose three parallel solutions to integrate these categories into WordNet in this work.

Solution 1: Leveraging on the subclassOf. The taxonomy of Wikidata is contributed by adding the “subclassOf” that is related to the hypernyms relationship in the taxonomy of WordNet. Referred to [62], we link Wikidata leaf node concepts to the WordNet by leveraging the “subclassOf”.

Solution 2: Parsing the Concept. Referred to the previous work [23], we can also link the concept to the WordNet through word parsing. For example, for the concept *Sumatran Orangutan*, we parse this concept [31] and get its head compound “Orangutan”. In this way, we add *Sumatran Orangutan* as the new hyponym of the “Orangutan” if “Orangutan” exists in WordNet.

Solution 3: Linking to the Closed Synset. We calculate the word embedding of both the synsets and given concepts through Spacy [31]. If a given concept cannot be linked to WordNet, we add this category to the hyponym of its nearest cosine distance synset.

1. The complete list of public datasets is reported in *Supplementary Material*.

3.3 Concepts Tagging

Visuality. Yang *et al* has mentioned the non-visual category problem in their work [72]. We illustrate visual and non-visual words in Fig. 2. To mitigate this problem, we conduct visual concept tagging for our build label system. Specifically, a concept is non-visual if three out of five annotators think this word is less concrete, and its sample images can rarely imply a common semantic meaning. We illustrate the concept tagging in Fig. 3(a).

Commonality. Based on the visual concepts, we further conduct common concept annotation for all visual concepts. Referred to COCO [44], “common concept” refers to entry-level categories that are commonly used by humans when describing objects (*e.g.* dog, chair, person). Specifically, a concept is positive only if it receives at least three-fifths of the votes. Based on the proposed annotation method, we retain 809 common concepts for the annotation of object detection.

4 ACTIVE DATASET CONSTRUCTION - BAMBOO

Equipped with the unified and comprehensive label system, we start to construct Bambooactively. In this section, we first introduce the active learning pipeline for building Bamboo in Sec 4.1. We summarize this pipeline in Algorithm 1. Then in Sec. 4.2, we discuss the superiority of our newly proposed active learning methods—we are the **first** time beat the random sampling in selecting the most valuable data for data pre-training.

Algorithm 1: Outline of AL Framework

```

input : Raw unlabeled pool  $\Theta$ ; Number of active
         learning rounds  $T$ ; Neural network  $\phi$ ;
 $\mathcal{P}^L(0) \leftarrow$  Annotating a few data from  $\Theta$  and
         adding all inherited data as cold start;
 $\mathcal{P}^U(0) \leftarrow \Theta - \mathcal{P}^L(0) \cap \Theta$ ;
         Initializing model  $\phi(0)$  based on  $\mathcal{P}^L(0)$ ;
for  $r \leftarrow 1$  to  $T$  do
     $\mathcal{P}^R(r) \leftarrow$  Rectifying  $\mathcal{P}^U(r-1)$  w/  $\phi(r-1)$ ;
     $\mathcal{S}^U(r) \leftarrow$  Sampling in  $\mathcal{P}^R(r)$  w/  $\phi(r-1)$ ;
     $\mathcal{S}^L(r) \leftarrow$  Annotating valid data from  $\mathcal{S}^U(r)$ ;
     $\mathcal{P}^U(r) \leftarrow \mathcal{P}^U(r-1) - \mathcal{S}^U(r)$ ;
     $\mathcal{P}^L(r) \leftarrow \mathcal{P}^L(r-1) \cup \mathcal{S}^L(r)$ ;
    Training  $\phi(r)$  on  $\mathcal{P}^L(r)$ ;
end
    
```

4.1 Active Learning Framework

4.1.1 Building Unlabeled Data Pool

For image classification, one query word has one visual concept mentioned in Sec. 3.3. For object detection, one query has two concepts, *i.e.*, common concept + scene semantic word or common concept + common concept. For example, *dog + street* or *dog + ball*. To further enrich the searching results, any given query word can be converted to its synonyms or its Chinese, Spanish, Dutch and Italian version for querying. Totally, we obtain a 170M unlabeled pool for classification and a 200M unlabeled pool for detection.

2. This step is not included in the current active learning research.

(a) **Visuality and Commonality**

Visuality

Is **Parliamentarian** a visual concept? Yes No
 Description: An elected member of the British Parliament ...

Reference Image

<https://www.google/mag> <https://www.goog> <https://www.goog>

Commonality

Is **WillowFlute** a Common concept? Yes No
 Description: Nordic folk flute...

Reference Image

<https://www.google/mag> <https://www.goog> <https://www.goog>

(b) **Image Classification and Object Detection**

Image Classification

Is this a **Golden Retriever**? Yes No
 Description: An English breed having a long silky golden coat.

Unlabeled Image Reference Image

<https://www.flickr> <https://www.goog> <https://www.goog>

Object Detection

Your choice: Normal bbox Group bbox Invalid Image

Reference Image

<https://www.flickr> <https://www.goog> <https://www.goog>

Pseudo Label: Person Description: A human being Annotator_1

Pseudo Label: Car Description: A motor vehicle... Annotator_2

Fig. 3. **User interfaces for concept tagging and annotation.** (a) The meta information of the concept tagging consists of tags, descriptions, and reference images. (b) Interface for image classification and object detection. For the object detection task. The image is assigned to different annotators based on its multiple pseudo labels. In addition, annotators should choose the attribute of the bounding box. The criteria for the attribute options are described in detail in *Supplementary Material*.

4.1.2 *Cold Start*

Cold start is the very first step for active learning. The labeled data pool $\mathcal{P}^L(0)$ to initialize the model $\phi(0)$ for the cold start phase include two parts as follows.

Public Dataset. As mentioned in Sec. 3.1, we use 24 datasets as concept resources, including 19 image classification datasets and 5 object detection datasets. Referred to the evaluation suite of popular transfer learning study [29], [38], [77], we select 12 datasets for downstream evaluation. We include the annotation of the other 12 datasets—9 image classification datasets and 3 object detection datasets. In total, we inherit 27,848,477 classification annotations and 21,983,223 object bounding box annotations from those 12 datasets.

New Annotated Data. For concepts not included in public datasets, we sample images from unlabeled pool Θ and annotate data for them until they have 50 annotated data.

4.1.3 *OOD Rectification*

Image Classification. In this step, we rectify the latest unlabeled data pool $\mathcal{P}_C^U(r-1)$. As shown in Fig 4 (b), in each round r , we firstly utilize $\phi_C(r-1)$ trained on $\mathcal{P}_C^L(r-1)$ to acquire predictions of each image in $\mathcal{P}_C^U(r-1)$. We infer an image is out-of-distribution if its top-5 predicted categories do not overlap with its related categories. Specifically, we define the related categories of an image as the sub-population of hypernyms of its query word. If an image is not out-of-distribution, we add it into $\mathcal{P}_C^R(r)$ for further data sampling. In Sec. 4.2, we empirically observe that OOD rectification is essential for AL to function in realistic scenarios.

Object Detection. Similar to classification, we acquire proposal predictions of each image in $\mathcal{P}_D^U(r-1)$ by $\phi_D(r-1)$.

On the one hand, we filter out the image with less than two proposals. Such images might be noisy data or semantic shift data. On the other hand, we filter out the image with more than 15 identical semantic proposals since such image might be the covariate shift data. As shown in Fig 4 (b), the remaining in-distribution data forms $\mathcal{P}_D^R(r)$ for the data sampling.

4.1.4 *Data Sampling.*

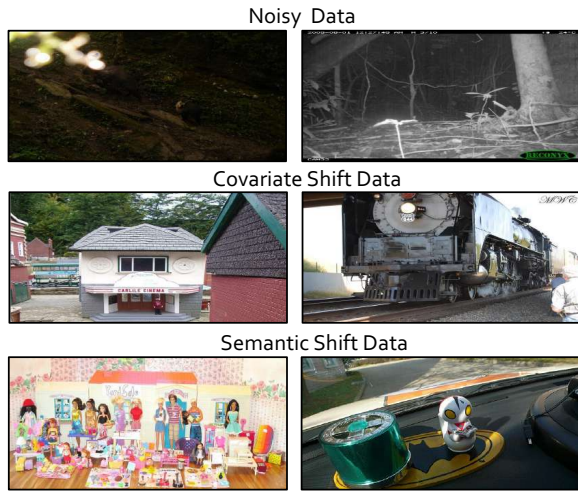
In this step, we use ClusterMargin [17], which considers both the uncertainty and diversity in data, to select the most valuable data $S^U(r)$ from the latest rectified data pool $\mathcal{P}^R(r)$ for annotation.

4.1.5 *Data Annotation.*

Finally, we rely on an online platform to annotate valid data—its querying word accurately describes the semantic meaning of this data—in $S^U(r)$, forming the labeled data set $S^L(r)$. We illustrate our online platform in Fig. 3, and introduce the details of annotations as follows. **Image Classification.** To provide a comprehensive definition of each category, we construct reference images that are collected by querying Google image search and Wikipedia [21]. For each image in $S^U(r)$, its meta-information has two parts: the query word of this image and the reference images of the query word. We then ask the five annotators whether this image conforms to its meta information. An image is annotated and added into $S^L(r)$ —valid data—only if at least 3 out of 5 annotators give the positive answer to the question as mentioned above.

Object Detection. Following Objects365 [59], one annotator is responsible for annotating a specific category, which improves the annotation efficiency and quality. Similar to

(a) OOD Samples (query word: "person")



(b) OOD Rectification

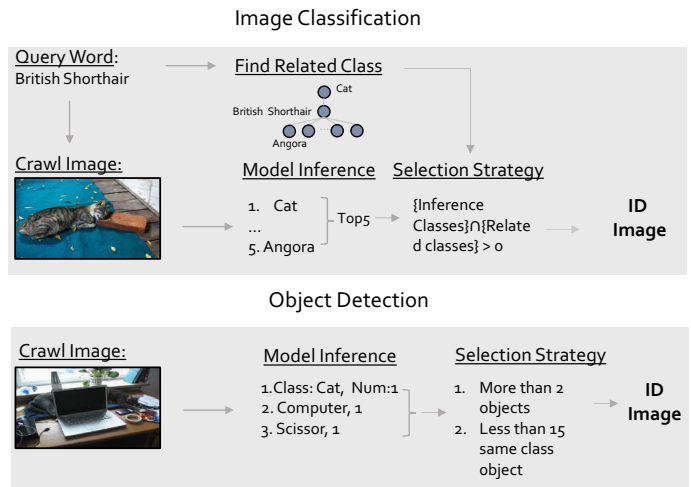


Fig. 4. (a) The illustration of out-of-distribution (OOD) data in realistic scenarios. Mainly, three types of OOD data exist in the unlabeled data pool, including noisy data, covariate shift data (*i.e.*, OOD samples from a different domain), and semantic shift data (*i.e.*, OOD samples are drawn from different classes). (b) The illustration of OOD rectification. OOD rectification filters OOD data in the unlabeled data pool, which is crucial for active learning.

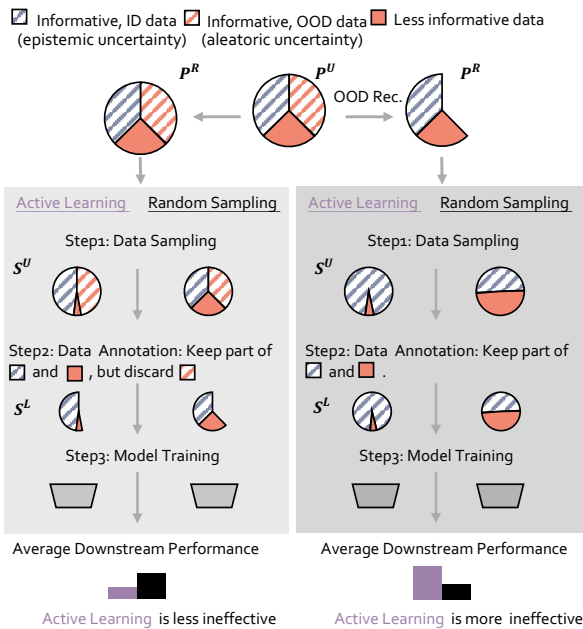


Fig. 5. The Illustration of how our OOD rectification step helps active learning performs better in realistic scenarios.

OpenImages [41], meta information of an image includes not only its reference images but also its pseudo labels that include i) the query words of this image. ii) the category predictions of available detection models. iii) re-labeling predictions [76] of the latest trained classification model ϕ_C .

4.2 Studies on Active Annotation

In academic active learning (AL) works [17], [32], researchers conduct data sampling on the leave-out “unlabeled” data pool that are separated from a curated dataset, *e.g.* ImageNet [17] and CIFAR10 [54]. All the data in this

“unlabeled” data pool is strictly valid.³ However, in realistic annotation scenarios, the real unlabeled data pool is composed of valid data and invalid data that is mostly out-of-distribution data, as shown in Fig. 4(a). Therefore, can AL methods are effective when the invalid data in the unlabeled data pool is an open question. And we found that:

Current Active Learning Methods are Ineffective for Sampling Valuable Data in the Real unlabeled data pool.

As shown in Fig. 6(a), we illustrate the number of $S^L(1)$ (the first round valid data set of Bamboo) when $\mathcal{P}^R(1) \leftarrow \mathcal{P}^U(0)$ (the academic active learning framework). We observe that AL sampling would retain fewer data in $S^L(1)$ than random sampling. For example, Entropy Sampling selects 70% less data than random sampling, resulting in worse downstream performance.

The Devils are in Uncertainty Modeling. As discussed in [20], [36], there are mainly two types of uncertainty for the deep models: *Aleatoric* and *Epistemic*. Both uncertainties are informative, but the aleatoric uncertainty is the out-of-distribution data, and the epistemic uncertainty is the in-distribution data. Considering $\mathcal{P}^U(0)$ where aleatoric-uncertain data, epistemic-uncertain data, and other less-informative data exist, when $\mathcal{P}^R(1) \leftarrow \mathcal{P}^U(0)$, $S^U(1)$ under AL sampling would have more aleatoric-uncertain data than that under random sampling, as AL methods tend to select uncertain data. Eventually, $S^L(1)$ under AL sampling should has less data than that under random sampling as aleatoric uncertain data is invalid for annotators. We illustrate this phenomenon in Fig. 5 left. As shown in Fig. 6 (a), with much less $S^L(1)$, AL methods’ performances are hence worse than RS.

OOD Rec. Boosts AL Performance. When $\mathcal{P}^R(1) \leftarrow$ Rectifying $\mathcal{P}^U(0)$ w/ $\phi(0)$ (our active learning framework), our proposed OOD rectification filters out the aleatoric uncertain data in $\mathcal{P}^U(0)$. Therefore, $\mathcal{P}^R(1)$ is only comprised of

3. Annotator had deleted invalid data as dataset established.

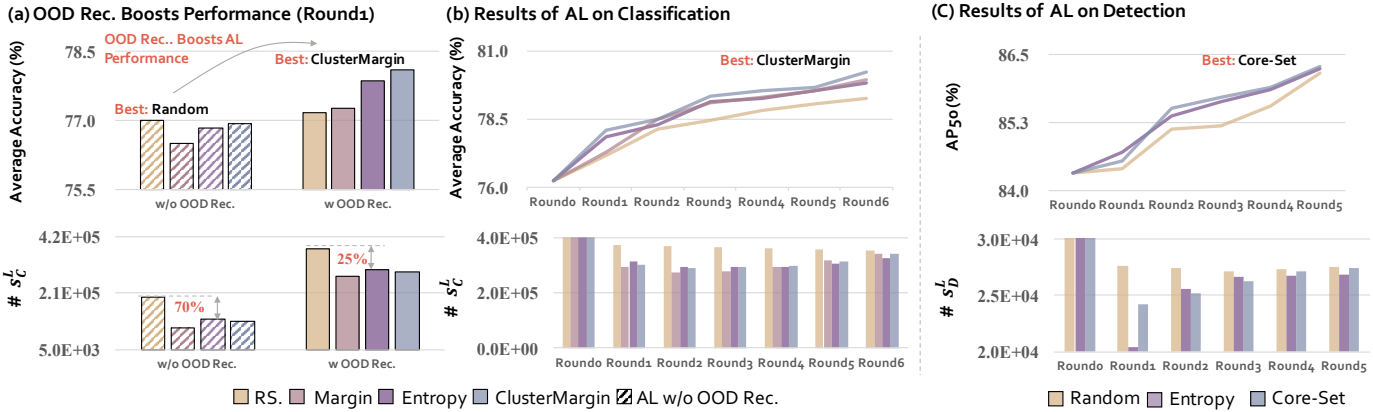


Fig. 6. **The study of active annotation in Bamboo.** (a) current AL methods struggle in realistic scenarios. Random sampling achieves better performance than each AL method. *OOD Rectification* boosts all AL methods to outperform random sampling. AL methods are still more helpful for model training with less valid data. It implies that the valid data that AL methods selected are much more informative. (b) and (c) in both classification and detection tasks, AL methods (ClusterMargin and Core-Set) that consider both the uncertainty and diversity select the most valuable data for model training. s_C^L refers annotated valid data from a given AL batch. Average accuracy denotes the average performance of models on the downstream datasets.

epistemic-uncertain data—which is informative—and other less-informative data. Since AL methods would select more epistemic uncertain data in $\mathcal{P}^R(1)$ than random sampling, they eventually perform better. We illustrate how OOD rectification helps active learning performs better in realistic scenarios in Fig. 5 right. As shown in Fig. 6(b,c), with OOD rectification, in both classification and detection tasks, AL methods (ClusterMargin and Core-Set) that consider both the uncertainty and diversity select the most valuable data for model training.

5 DATASET STATISTICS

As shown in Fig. 7, we illustrate the sorted distribution of image numbers per category in the Bamboo. Generally, we emphasize that the new annotated data in the Bamboo-CLS and Bamboo-DET are a powerful complement to the current public datasets—This data mostly belongs to tail classes of public datasets and new classes. In the following, we briefly describe the data statistics of Bamboo.

Image Classification (Bamboo-CLS). Bamboo-CLS has 68,884,828 images spread across 119,035 categories. 42,648,217 out of 68,884,828 images are newly annotated, which is twice of ImageNet22K. In addition, 20,000 out of 119,035 categories are from Wikidata. These categories mainly are fine-grained concepts, such as *Folland Midge* (one type of fighter) and *hemaria hemishphaerica* (a species of fungi). To our knowledge, Bamboo-CLS is the largest clean image dataset available to the vision research community, in terms of the total number of images and categories.

Object Detection (Bamboo-DET). Bamboo-DET has 3,104,012 images across 809 categories. Specifically, 557,457 images are newly annotated, and 150 concepts are from the Wikidata. In addition, we provide the statistics on instances per image of Bamboo-DET. As shown in Table 1, Our newly annotated data has 8.3 instances (on average) per image, which is dense than existing datasets, *i.e.* MS-COCO, Object-365, and OpenImages.

6 EXPERIMENTS

6.1 Experimental Setups

6.1.1 Upstream Pre-training

Hyper-parameter. We train the models on 64 A100 GPUs for image classification, with a total batch size of 8,192. We employ an AdamW [45] optimizer of 30 epochs using a cosine decay scheduler with two epochs of linear warm-up. The ResNet-50 backbone is initialized from the model officially offered by PyTorch. The ViT B/16 backbone is initialized from ImageNet1K model provided by timm.⁴ The weight decay, and warm-up learning rate are 2×10^{-8} , 10^{-6} , and 2×10^{-2} .

Datasets. Beyond the new annotated data, we include ImageNet22K [18], INaturalist2021 [65], Herbarium2021,⁵ Danish Fungi 2020 [52], iWildCam2020 [4], TsinghuaDogs [82], Places [80], FoodX-251 [35], CompCars [74] in the upstream classification dataset training. We train the models on 48 A100 GPUs for detection, with a total batch size of 384, a total learning rate of 0.4, SGD optimizer of momentum 0.9, and a weight decay of 0.0001. We use the MultiStep learning rate scheduler with the decay rate of 0.1 on [16, 22] epochs and train for 26 epochs in total. We also applied the warm-up learning rate of 0.0004 for 1 epoch. We used Cross-Entropy-Loss for categorization and Smoothed-L1-Loss for bounding box regression. Beyond the new annotated data, we include COCO [44], Objects365 [59] and OpenImages [41] in the upstream object detection dataset training.

6.1.2 Downstream Evaluation

Datasets. In the following sections, we adopt the downstream datasets that are widely used in the transfer learning study [29], [38], [77]. For models pre-trained on the image classification datasets, we use CIFAR10 [40], CIFAR100 [40], OxfordFlower [50], Food101 [7], Caltech101 [24], Oxford-Pets [51], DTD [16], StanfordCars [39], FGVC-Aircraft [47],

4. <https://github.com/rwightman/pytorch-image-models/tree/master/timm>

5. <https://www.kaggle.com/c/herbarium-2021-fgvc8/overview>

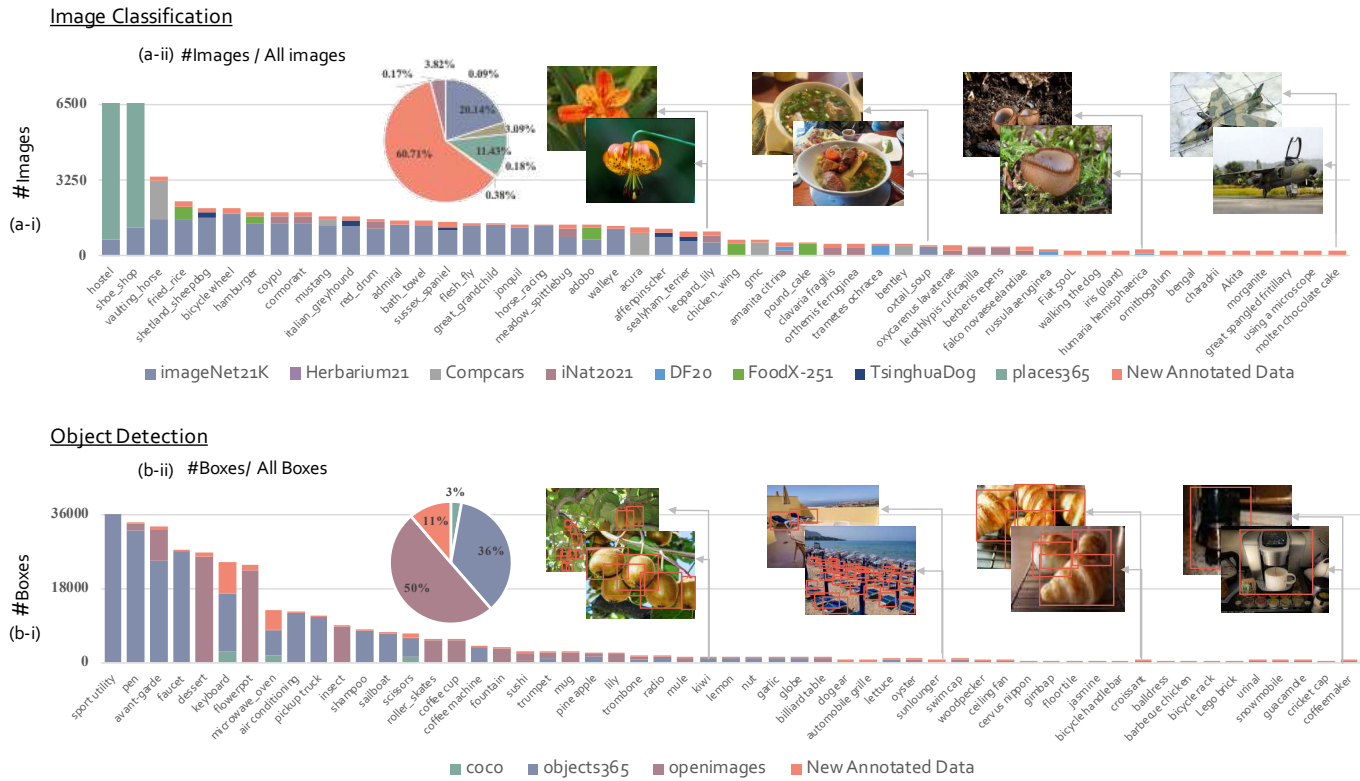
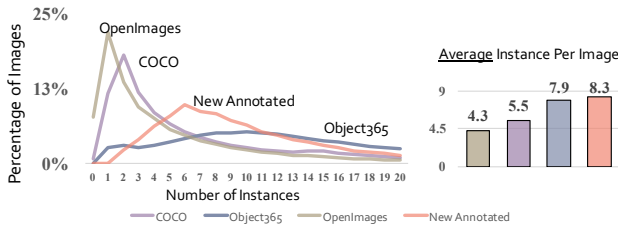


Fig. 7. **Sorted distribution of image number per category in the Bamboo.** (a-i) Bamboo-CLS contains 68,884,828 images spread across 119,035 categories. Category names are shown for every 250 intervals. Bamboo-CLS includes some fine-grained concepts that not be included in the current public datasets, such as *Folland Midge*. (a-ii) The new classification annotated data accounts for 60.71% of images in Bamboo. (b-i) Bamboo-DET contains 3,104,012 images across 809 categories. Category names are shown for every 16 intervals. (b-ii) The new detection annotated data accounts for 11% of images in Bamboo.

TABLE 1

Left: The statistics of the number of bounding boxes per image. Quantitatively, our new annotated data has 8.3 instances (on average) per image, which is more dense compared with the other datasets like COCO and OpenImages. **Right: Summary of Bamboo.** Bamboo is the largest fully annotated vision dataset available to the general research community, in terms of the total number of images, the number of concepts, and the number of bounding boxes (for object detection task).



Datasets	Concepts	Images	Boxes	Anno.
YFCC-100M [63]	-	100M	-	No
ImageNet22K [18]	22K	14M	-	Yes
Bamboo-CLS	119K	69M	-	Yes
COCO [44]	80	118K	1M	Yes
Objects365 [59]	365	609K	10M	Yes
OpenImages [41]	600	2M	14M	Partial
Bamboo-DET	809	3M	27M	Yes

SUN397 [69], ImageNet1K [55] as the downstream evaluation datasets. As for the object detection task, we select PASCAL VOC [22] and CityPersons [79] as the downstream evaluation datasets. These datasets cover a wide range of image domains. The number of images in each dataset ranges from 2,000 to 80,000, and the number of classes in each dataset ranges from 10 to 8,000.

Evaluation Protocol. For the classification task, we use image features taken from the penultimate layer of each model, ignoring any classification layer provided. We train a logistic regression classifier for the linear probe evaluation setting. We finetune the entire model loaded with its backbone and FPN weights for the detection task. We only report the evaluation performance of models on downstream datasets.

We finetune the model on 8 1080-Ti GPUs for detection, with the batch size of 16, SGD optimizer of momentum 0.9, and weight decay 0.0001 by loading the weights of backbone and FPN. We conduct a grid search on learning rate among $[5 \times 10^{-4}, 1 \times 10^{-3}, 5 \times 10^{-3}, 1 \times 10^{-2}]$. The learning rate is decayed by 0.1 at 16 and 18 and stopped training at 19 epochs.

6.2 Power of Bamboo as Pre-Training

6.2.1 Main Results

Information-Dense Annotations Matter. As shown in Table 2, ResNet-50 (RN50) pre-trained on CLIP (400M) or IG-1B (1B) achieves better downstream task performance

TABLE 2

Downstream classification tasks performance among different pre-training methods. Bamboo achieves the state-of-the-arts linear probe performance on the downstream tasks. Lang. indicates image-text pair. Numbers in red are the performance gain on the same backbone network. Bamboo here refers to the Bamboo-CLS. Pets indicates OxfordPets. Flowers indicates OxfordFlower. Cars indicates StanfordCars. Aircraft indicates FGVC-Aircraft. IN1K indicates ImageNet1K. Results reported by the author are marked in gray. We mainly compare with the methods conducted on supervised learning. Other performance of current methods are also presented.

Method	Data	Annotation	Model	Paradigm	CIFAR10	CIFAR100	Food101	Pets	Flowers	SUN397	Cars	DTD	Caltech101	Aircraft	IN1K	AVG†
SwAV [10]	IN1K	1.2M	RN50	Self.	92.5	76.6	76.4	88.0	93.0	65.5	60.5	78.1	91.0	56.0	66.9	76.8
DINO [11]	IN1K	1.2M	RN50	Self.	93.7	79.2	77.2	89.2	96.2	66.0	68.3	77.6	92.3	63.1	83.3	79.8
SWSL [71]	IG-1B	1B	RN50	Semi.	94.7	79.5	79.1	94.4	94.6	67.8	65.9	77.8	96.1	58.4	81.2	80.9
WSL [46]	IG-1B	1B	RX101	Weak.	95.0	78.2	83.5	95.5	90.8	67.9	72.3	75.3	93.3	53.9	83.3	81.0
CLIP [53]	WIT	400M	RN50	Lang.	88.7	70.3	86.4	88.2	96.1	73.3	78.3	76.4	89.6	49.1	73.3	79.1
CLIP [53]	WIT	400M	B/16	Lang.	96.2	83.1	92.8	93.1	98.1	78.4	86.7	79.2	94.7	59.5	80.2	85.6
BiT [37]	IN1K	1.2M	RN50	Sup.	91.7	74.8	72.5	92.3	92.0	61.1	53.5	72.4	91.2	52.5	75.2	73.6
BiT [37]	IN22K	14M	RN50	Sup.	94.9	82.2	83.3	91.5	99.4	69.9	59.0	77.3	93.9	55.6	76.7	80.3
RN50	Bamboo	69M	RN50	Sup.	93.9	81.2	85.3	92.0	99.4	72.2	91.1	76.5	93.2	84.0	77.2	86.0 (+5.1)
B/16	Bamboo	69M	B/16	Sup.	98.2	90.2	92.9	95.1	99.8	79.0	93.3	81.2	97.0	88.1	83.6	91.8 (+6.2)

TABLE 3

Comparisons of downstream detection tasks performance.

Pre-trained model on Bamboo achieves significant performance gain. Bamboo here refers to the Bamboo-DET. VOC means the PASCAL VOC dataset [22]. CITY. means the CityPersons dataset [79].

Data	Anno.	VOC AP50 ↑	CITY. MR ↓	COCO mmAP ↑
COCO [59]	1M	85.1	16.2	-
OpenImages [59]	14M	82.4	16.8	37.4
Objects365	10M	86.4	14.7	39.3
Bamboo	27M	87.5 (+1.1)	12.6 (+2.1)	43.9 (+4.4)

than BiT pre-trained on ImageNet1K (IN1K) [55]. However, compared to RN50 pre-trained on Bamboo, CLIP-RN50 or RN50 pre-trained on IG-1B achieves inferior performance.

It indicates that the amount of informative-dense annotations instead of the sheer number of annotations is much more essential for model pre-training. Compared to CLIP, which leverages the vast amount of image-text pairs on the web for pre-training, our Bamboo presents an active and continual framework that collects and annotates fully-supervised samples in a highly scalable manner.

Comprehensive Label System Helps. As shown in Table 2, most methods pre-trained on IN1K, IG-1B, or WIT achieve more than 90% accuracy on the OxfordPets and OxfordFlower. But they only achieve less than 80% accuracy on the StanfordCars and FGVC-Aircraft. It indicates that these pre-trained datasets might include more semantic concepts related to OxfordPets and OxfordFlower. Our BambooTX spreads a large spectrum of concepts. Notably, it includes much more concepts that are neglected in the current public and nonpublic datasets. As a result, models pre-trained on Bamboo achieve much better performance than other methods. Beyond general object detection, it is also important to validate the generalization ability on specific object detection problems like pedestrian detection.

Bamboo is an Effective Pre-Training Source. Compared to other methods, Bamboo achieves the best performance among downstream tasks on average. As shown in Table 2, ViT B/16 pretrained on Bamboo outperforms CLIP with

6.2 points gain. It indicates that our annotation is much more informative and hence more helpful for the model pre-training. In addition, Table 3 presents that ResNet-50 with FPN pretrained on Bamboo outperforms Objects365 with 1.1 points gain on PASCAL VOC and 2.1 points gain on CityPersons.

6.2.2 Further Analysis

The Influence Of Similar Semantic Proposals. The total annotation cost for the object detection task depends on the number of proposals. Images with dense proposals are more expensive than sparse ones. Based on our observation, many proposals with similar semantics tend to form a group in a single image. To evaluate their effectiveness, we conduct the following experiments on Objects365 [59] dataset.

Firstly, we define an image as a crowded image if it contains at least one category with more than 15 proposals. By removing all 27K crowded images from the full Objects365 dataset, we denote the remaining part as Objects365-sparse. Keeping the number of proposals the same as Objects365-sparse, we randomly removed 90K images from the full Objects365 dataset and marked the remaining part as Objects365-random. Furthermore, keeping the total object amount the same as Objects365-sparse, we randomly removed 101K non-crowded images from the full Objects365 dataset and denoted the remaining part as Objects365-dense.

Dataset	Images	Proposals	VOC AP50 ↑
Objects365-sparse	581K	8.2M	86.3
Objects365-random	519K	8.2M	85.8
Objects365-dense	508K	8.2M	85.1

Given the same annotation budget, we find that choosing to label non-crowded images yields better results for pre-training performance. Therefore, as mentioned in Sec. 3.3.2 of the main paper, we filter out covariate shift data in the OOD rectification step.

Finetuning Transfer. We compared our model pre-trained on Bamboo to various with the ResNet-50 backbone. We

TABLE 4

Comparisons of zero-shot downstream classification tasks performance among different pre-training methods. Bamboo achieves the state-of-the-arts linear probe performance on the downstream tasks. Lang. indicates image-text pair. Numbers in red are the performance gain on the same backbone network. Bamboo here refers to the Bamboo-CLS. Pets indicates OxfordPets. Flowers indicates OxfordFlower. Cars indicates StanfordCars. Aircraft indicates FGVC-Aircraft. IN1K indicates ImageNet1K. Results reported by the author are marked in gray. We mainly compare with the methods conducted on supervised learning. Other performance of current methods are also presented.

Method	Data	Annotation	Model	Paradigm	CIFAR10	CIFAR100	Food101	Pets	Flowers	SUN397	Cars	DTD	Caltech101	Aircraft	IN1K	AVG \uparrow
CLIP [53]	WIT	400M	RN50	Lang.	91.6	68.7	89.2	88.9	70.4	65.2	65.6	46	89.3	27.1	68.6	70.0
RN50	Bamboo	69M	RN50	Sup.	93.8	67.7	81.6	74.3	87.3	58.7	63.0	51.1	88.4	87.2	82.5	76.0 (+6.0)

TABLE 5

Comparisons of fine-tuning downstream classification tasks performance among different pre-training methods. Bamboo achieves the state-of-the-arts fine-tuning performance on the downstream tasks.

Method	Data	Annotation	Model	Paradigm	CIFAR10	CIFAR100	Food101	Pets	Flowers	SUN397	Cars	DTD	Caltech101	Aircraft	IN1K	AVG \uparrow
DINO	IN1K	1.2M	RN50	Self.	97.1	84.0	86.3	90.0	96.1	65.2	84.6	77.6	91.4	81.8	66.5	83.7
SWAV	IN1K	1.2M	RN50	Self.	97.2	84.2	86.0	90.3	95.7	64.4	83.9	77.2	91.7	81.2	66.9	83.5
SWSL	IG-1B	1B	RN50	Semi.	97.0	86.5	87.3	94.4	97.0	66.0	88.5	78.3	93.8	84.0	81.7	86.8
BiT-S	IN1K	1.2M	RN50	Sup.	97.0	85.0	85.7	92.8	95.0	60.3	87.5	74.7	92.0	83.8	75.2	84.5
BiT-M	IN22K	14M	RN50	Sup.	97.6	86.2	87.9	91.5	98.1	64.2	88.2	78.4	92.9	84.3	76.7	86.0
RN50	Bamboo	69M	RN50	Sup.	97.3	87.0	87.5	92.0	99.4	72.2	91.4	77.1	93.9	85.9	77.1	87.3 (+0.5)

present the finetuning transfer performance of the models pre-trained on Bamboo. The finetuning strategy among each downstream task is followed by the SimCLR [13]. Table 5 shows the comparison. Bamboo model achieves a 1.3% average accuracy gain compared to BiT-M pre-trained on the current largest public classification dataset: ImageNet22K. It indicates a larger, carefully annotated dataset can continually improve the performance of models. Besides, Bamboo model achieves a 0.5% average accuracy gain compared to SWSL, pre-trained on the IG-1B with 1B weakly supervised hashtags. Bamboo is 20 times smaller than IG-1B, which indicates that the amount of informative-dense annotations instead of the sheer number of weak annotations is much more essential for model pre-training.

Zero-Shot Transfer. We present the zero-shot transfer performance of the models pre-trained on Bamboo. We compared our model pre-trained on Bamboo to CLIP models with the same backbone.

Table 4 shows the comparison. We can indicate that Bamboo model conclusively outperforms CLIP model with the same backbone: RN50. Specifically, Bamboo model achieves a 6% average accuracy gain. On the FGVC-Aircraft, Bamboo model achieves 87.2%, despite having never seen any training images from this dataset. Bamboo includes all the concepts in the downstream tasks. However, we conduct data overlap analysis of Bamboo in Sec. 7, ensuring Bamboo rarely includes downstream data.

Robustness to Natural Distribution Shift. We conduct experiments on the ObjectNet [2] to compare Bamboo models with other models when evaluated on the data with controls for rotation, background, and viewpoint. ObjectNet is a dataset collected in the real world, where multiple objects are always present. There are 313 object classes in total,

with 113 overlapping with ImageNet1K. We follow the literature [37], [53] and evaluate our models on those 113 classes.

Method	Data	Model	Para.	ObjectNet \uparrow
BiT-L [37]	JFT-300M	RN50	Weak.	37.6
ANN-1.3B [3]	ANN-1.3B	B/16	Weak.	50.7
RN50	Bamboo	RN50	Sup.	38.8 (+1.2)
B/16	Bamboo	B/16	Sup.	53.9 (+3.2)

As shown above, we compare Bamboo models with the state-of-the-art model with the same backbone. Specifically, ResNet-50 pre-trained on Bamboo achieves 1.2% gains compared with ResNet-50 pre-trained on JFT-300M. ViT B/16 pre-trained on Bamboo achieves 3.2% gains compared with ViT B/16 pre-trained on Anno-1.3B. Even though JFT-300M and Anno-1.3B are much larger than Bamboo, the informative data in Bamboo is more helpful for pre-trained models in real scenarios.

7 SOCIAL IMPACT

The proposed Bamboo dataset and pre-training model shows the capacity and generalization of learned image representation which could benefit many applications of computer vision. However, our data usage might bring several risks, such as data overlapping, privacy, and inappropriate content. We discuss these risks and their mitigation strategies as follows.

Data Overlapping. A concern with pre-training on an extensive dataset is unintentional overlap with downstream evaluation [53]. To enable a meaningful test of generalization, we identify and remove all duplicates among upstream data. Specifically, we utilize Difference Hash (DHash) [5]

to present the information of each image. We calculate the hash-code of each downstream image and each crawled image, and two images with the same hash-code are regarded as similar ones. Then, we filter out the crawled images that are similar to downstream images. Based on the above method, we discard 122,939 images for classification and 1,046 images for detection from the unlabeled pool.

Copyright. We crawl only the data under the Creative Commons license (CC-BY) for the Bamboo-DET. This license allows free use, redistribution, and adaptation for non-commercial purposes. For the Bamboo-CLS data, 30% of data is under the CC-BY license because of its large volume of data. For Bamboo-CLS data that is not under the CC-BY license, referred to LAION-400M [56] and Conceptual 12M [12], we only present the lists of URLs to this data without redistribution. We build the meta file as follow.

[image_url] [class_index]

Referred to *Authors Guild, Inc. v. Google Inc.* [8], training data on the copyrighted works might be considered as transformative uses and was thus might be regarded as *Fair Use*⁶. In addition, referred to *Article 30-4 of the new Copyright Act* [1], there are no restrictions on the subject, purpose, and method of data analysis, and there is no obligation to compensate the copyright holder. However, we admit that using copyright material as training data is still a controversial issue in Artificial Intelligence, and we would no doubt follow the newest law worldwide. Bamboo is specifically open for non-commercial research and/or educational purposes to respect the copyright law. For researchers and educators who wish to use copyrighted images for that purpose, training or benchmarking models with copyrighted works would be qualified as *transformative* uses and thus not infringe copyright law in the U.S.⁶ Nevertheless, the users must strictly follow the Flickr Terms of Use.⁷ And the users of these images accept full responsibility for the use of the image.

Problematic Content. The inappropriate contents such as drugs, nudity, and other offensive content exist in the web data. we ask annotators to discard such images instead of conducting annotation.

Privacy. To mitigate privacy issues with public visual datasets, researchers have attempted to obfuscate private information before publishing the data [25], [73]. We plan to follow this line of work to blur faces, and license plates in our new annotated data. In addition, if the original picture found at the URL present on the Bamboo on the record states users' names, phone numbers, or any personal information, users can request a takedown of this image.

Bias. The images were crawled from Flickr, thus inheriting all the biases of that website. The usage of user-generated data might bring the risk of bias. We plan to tackle this problem by balancing various categories.

8 CONCLUSION

In our work, with a human-machine synergy, we actively and continually build a mega-scale and information-dense

dataset, namely Bamboo. Bamboo is the largest clean image dataset available to the vision research community, in terms of the total number of images and the number of categories, for classification and detection tasks. Our key insight is that a unified and visually-oriented label system is crucial for model pre-training, and rectifying OOD samples is indispensable for AL to function in realistic scenarios. We have demonstrated the effectiveness of Bamboo as a better pre-training dataset for various downstream tasks and provided several valuable observations.

REFERENCES

- [1] The act partially amending the copyright act (act no.52 of 2021; enacted may, 2021), 2010. 10
- [2] Andrei Barbu, David Mayo, Julian Alverio, William Luo, Christopher Wang, Danny Gutfreund, Joshua Tenenbaum, and Boris Katz. Objectnet: A large-scale bias-controlled dataset for pushing the limits of object recognition models. 2019. 9
- [3] Josh Beal, Hao-Yu Wu, Dong Huk Park, Andrew Zhai, and Dmitry Kislyuk. Billion-scale pretraining with vision transformers for multi-task visual representations. *arXiv preprint arXiv:2108.05887*, 2021. 9
- [4] Sara Beery, Arushi Agarwal, Elijah Cole, and Vighnesh Birodkar. The wildcam 2021 competition dataset. *arXiv preprint arXiv:2105.03494*, 2021. 6
- [5] Hoyt Ben. Duplicate image detection with perceptual hashing in python. <https://benhoyt.com/writings/duplicate-image-detection/#difference-hash-dhash>, 2017. 9
- [6] Rishi Bommasani, Drew A Hudson, Ehsan Adeli, Russ Altman, Simran Arora, Sydney von Arx, Michael S Bernstein, Jeannette Bohg, Antoine Bosselut, Emma Brunskill, et al. On the opportunities and risks of foundation models. *arXiv preprint arXiv:2108.07258*, 2021. 1
- [7] Lukas Bossard, Matthieu Guillaumin, and Luc Van Gool. Food-101 – mining discriminative components with random forests. In *ECCV*, 2014. 6
- [8] Victoria Campbell. Authors guild v. google, inc. *DePaul J. Art Tech. & Intell. Prop. L*, 27:59, 2016. 10
- [9] Mathilde Caron, Piotr Bojanowski, Armand Joulin, and Matthijs Douze. Deep clustering for unsupervised learning of visual features. In *ECCV*, pages 132–149, 2018. 2
- [10] Mathilde Caron, Ishan Misra, Julien Mairal, Priya Goyal, Piotr Bojanowski, and Armand Joulin. Unsupervised learning of visual features by contrasting cluster assignments. *arXiv preprint arXiv:2006.09882*, 2020. 1, 2, 8
- [11] Mathilde Caron, Hugo Touvron, Ishan Misra, Hervé Jégou, Julien Mairal, Piotr Bojanowski, and Armand Joulin. Emerging properties in self-supervised vision transformers. *arXiv preprint arXiv:2104.14294*, 2021. 8
- [12] Soravit Changpinyo, Piyush Sharma, Nan Ding, and Radu Soricut. Conceptual 12M: Pushing web-scale image-text pre-training to recognize long-tail visual concepts. In *CVPR*, 2021. 10
- [13] Ting Chen, Simon Kornblith, Mohammad Norouzi, and Geoffrey Hinton. A simple framework for contrastive learning of visual representations. In *ICML*, pages 1597–1607. PMLR, 2020. 2, 9
- [14] Xinlei Chen, Haoqi Fan, Ross Girshick, and Kaiming He. Improved baselines with momentum contrastive learning. *arXiv preprint arXiv:2003.04297*, 2020. 1
- [15] François Chollet. Xception: Deep learning with depthwise separable convolutions. In *CVPR*, pages 1251–1258, 2017. 2
- [16] M. Cimpoi, S. Maji, I. Kokkinos, S. Mohamed, , and A. Vedaldi. Describing textures in the wild. In *CVPR*, 2014. 6
- [17] Gui Citovsky, Giulia DeSalvo, Claudio Gentile, Lazaros Karydas, Anand Rajagopalan, Afshin Rostamizadeh, and Sanjiv Kumar. Batch active learning at scale. *arXiv preprint arXiv:2107.14263*, 2021. 1, 4, 5
- [18] Jia Deng, Wei Dong, Richard Socher, Li-Jia Li, Kai Li, and Li Fei-Fei. Imagenet: A large-scale hierarchical image database. In *CVPR*, pages 248–255. Ieee, 2009. 1, 3, 6, 7
- [19] Alexey Dosovitskiy, Philipp Fischer, Jost Tobias Springenberg, Martin Riedmiller, and Thomas Brox. Discriminative unsupervised feature learning with exemplar convolutional neural networks. *TPAMI*, 38(9):1734–1747, 2015. 2

6. <https://www.copyright.gov/fair-use/index.html>

7. <https://www.flickr.com/help/terms/api>

- [20] Daniel D’souza, Zach Nussbaum, Chirag Agarwal, and Sara Hooker. A tale of two long tails. *arXiv preprint arXiv:2107.13098*, 2021. **5**
- [21] Estimation lemma. Estimation lemma — Wikipedia, the free encyclopedia, 2010. [Online; accessed 29-September-2012]. **4**
- [22] Mark Everingham, Luc Van Gool, Christopher KI Williams, John Winn, and Andrew Zisserman. The pascal visual object classes (voc) challenge. *IJCV*, 88(2):303–338, 2010. **7, 8**
- [23] MS Fabian, Kasneci Gjergji, WEIKUM Gerhard, et al. Yago: A core of semantic knowledge unifying wordnet and wikipedia. In *WWW*, pages 697–706, 2007. **3**
- [24] Li Fei-Fei, Rob Fergus, and Pietro Perona. Learning generative visual models from few training examples: An incremental bayesian approach tested on 101 object categories. In *CVPR workshop*, pages 178–178. IEEE, 2004. **6**
- [25] Andrea Frome, German Cheung, Ahmad Abdulkader, Marco Zennaro, Bo Wu, Alessandro Bissacco, Hartwig Adam, Hartmut Neven, and Luc Vincent. Large-scale privacy protection in google street view. In *ICCV*, pages 2373–2380. IEEE, 2009. **10**
- [26] Yarin Gal. Uncertainty in deep learning. **1, 2**
- [27] Golnaz Ghiasi, Barret Zoph, Ekin D Cubuk, Quoc V Le, and Tsung-Yi Lin. Multi-task self-training for learning general representations. *arXiv preprint arXiv:2108.11353*, 2021. **1**
- [28] Ran Gilad-Bachrach, Amir Navot, and Naftali Tishby. Query by committee made real. *Advances in neural information processing systems*, 18, 2005. **1, 2**
- [29] Kaiming He, Haoqi Fan, Yuxin Wu, Saining Xie, and Ross Girshick. Momentum contrast for unsupervised visual representation learning. In *CVPR*, pages 9729–9738, 2020. **1, 2, 4, 6**
- [30] Kaiming He, Xiangyu Zhang, Shaoqing Ren, and Jian Sun. Deep residual learning for image recognition. In *CVPR*, pages 770–778, 2016. **2**
- [31] Matthew Honnibal and Ines Montani. spaCy 2: Natural language understanding with Bloom embeddings, convolutional neural networks and incremental parsing. To appear, 2017. **3**
- [32] Siyu Huang, Tianyang Wang, Haoyi Xiong, Jun Huan, and Dejing Dou. Semi-supervised active learning with temporal output discrepancy. In *ICCV*, pages 3447–3456, 2021. **5**
- [33] Juan Eugenio Iglesias, Ender Konukoglu, Albert Montillo, Zhuowen Tu, and Antonio Criminisi. Combining generative and discriminative models for semantic segmentation of ct scans via active learning. In *Biennial International Conference on Information Processing in Medical Imaging*, pages 25–36. Springer, 2011. **1, 2**
- [34] Ajay J Joshi, Fatih Porikli, and Nikolaos Papanikolopoulos. Multi-class active learning for image classification. In *CVPR*, pages 2372–2379. IEEE, 2009. **1, 2**
- [35] Parneet Kaur, Karan Sikka, Weijun Wang, Serge Belongie, and Ajay Divakaran. Foodx-251: A dataset for fine-grained food classification. *arXiv preprint arXiv:1907.06167*, 2019. **6**
- [36] Alex Kendall and Yarin Gal. What uncertainties do we need in bayesian deep learning for computer vision? *arXiv preprint arXiv:1703.04977*, 2017. **5**
- [37] Alexander Kolesnikov, Lucas Beyer, Xiaohua Zhai, Joan Puigcerver, Jessica Yung, Sylvain Gelly, and Neil Houlsby. Big transfer (bit): General visual representation learning. In *ECCV*, pages 491–507. Springer, 2020. **1, 8, 9**
- [38] Simon Kornblith, Jonathon Shlens, and Quoc V Le. Do better imagenet models transfer better? In *CVPR*, pages 2661–2671, 2019. **4, 6**
- [39] Jonathan Krause, Michael Stark, Jia Deng, and Li Fei-Fei. 3d object representations for fine-grained categorization. In *4th International IEEE Workshop on 3D Representation and Recognition (3dRR-13)*, Sydney, Australia, 2013. **2, 6**
- [40] Alex Krizhevsky, Geoffrey Hinton, et al. Learning multiple layers of features from tiny images. 2009. **1, 2, 6**
- [41] Alina Kuznetsova, Hassan Rom, Neil Alldrin, Jasper Uijlings, Ivan Krasin, Jordi Pont-Tuset, Shahab Kamali, Stefan Popov, Matteo Mallocci, Alexander Kolesnikov, et al. The open images dataset v4. *IJCV*, 128(7):1956–1981, 2020. **1, 3, 5, 6, 7**
- [42] Gustav Larsson, Michael Maire, and Gregory Shakhnarovich. Learning representations for automatic colorization. In *ECCV*, pages 577–593. Springer, 2016. **2**
- [43] Junning Li, Pan Zhou, Caiming Xiong, Richard Socher, and Steven CH Hoi. Prototypical contrastive learning of unsupervised representations. *arXiv preprint arXiv:2005.04966*, 2020. **2**
- [44] Tsung-Yi Lin, Michael Maire, Serge Belongie, James Hays, Pietro Perona, Deva Ramanan, Piotr Dollár, and C Lawrence Zitnick. Microsoft coco: Common objects in context. In *ECCV*, pages 740–755. Springer, 2014. **1, 3, 6, 7**
- [45] Ilya Loshchilov and Frank Hutter. Decoupled weight decay regularization. *arXiv preprint arXiv:1711.05101*, 2017. **6**
- [46] Dhruv Mahajan, Ross Girshick, Vignesh Ramanathan, Kaiming He, Manohar Paluri, Yixuan Li, Ashwin Bharambe, and Laurens Van Der Maaten. Exploring the limits of weakly supervised pretraining. In *ECCV*, pages 181–196, 2018. **2, 8**
- [47] S. Maji, J. Kannala, E. Rahtu, M. Blaschko, and A. Vedaldi. Fine-grained visual classification of aircraft. Technical report, 2013. **6**
- [48] George A Miller. *WordNet: An electronic lexical database*. MIT press, 1998. **2**
- [49] Ishan Misra and Laurens van der Maaten. Self-supervised learning of pretext-invariant representations. In *CVPR*, pages 6707–6717, 2020. **2**
- [50] M-E Nilsback and Andrew Zisserman. A visual vocabulary for flower classification. In *CVPR*, volume 2, pages 1447–1454. IEEE, 2006. **2, 6**
- [51] Omkar M Parkhi, Andrea Vedaldi, Andrew Zisserman, and CV Jawahar. Cats and dogs. In *CVPR*, pages 3498–3505. IEEE, 2012. **2, 6**
- [52] Lukáš Pícek, Milan Šulc, Jiří Matas, Jacob Heilmann-Clausen, Thomas S Jeppesen, Thomas Læssøe, and Tobias Froslev. Danish fungi 2020—not just another image recognition dataset. *arXiv preprint arXiv:2103.10107*, 2021. **6**
- [53] Alec Radford, Jong Wook Kim, Chris Hallacy, Aditya Ramesh, Gabriel Goh, Sandhini Agarwal, Girish Sastry, Amanda Askell, Pamela Mishkin, Jack Clark, et al. Learning transferable visual models from natural language supervision. *arXiv preprint arXiv:2103.00020*, 2021. **1, 2, 8, 9**
- [54] Dan Roth and Kevin Small. Margin-based active learning for structured output spaces. In *European Conference on Machine Learning*, pages 413–424. Springer, 2006. **1, 5**
- [55] Olga Russakovsky, Jia Deng, Hao Su, Jonathan Krause, Sanjeev Satheesh, Sean Ma, Zhiheng Huang, Andrej Karpathy, Aditya Khosla, Michael Bernstein, et al. Imagenet large scale visual recognition challenge. *IJCV*, 115(3):211–252, 2015. **7, 8**
- [56] Christoph Schuhmann, Richard Vencu, Romain Beaumont, Robert Kaczmarczyk, Clayton Mullis, Aarush Katta, Theo Coombes, Jenia Jitsev, and Aran Komatsuzaki. Laion-400m: Open dataset of clip-filtered 400 million image-text pairs, 2021. **10**
- [57] Ozan Sener and Silvio Savarese. Active learning for convolutional neural networks: A core-set approach. In *ICLR*. OpenReview.net, 2018. **1**
- [58] Burr Settles. Active learning literature survey. 2009. **1, 2**
- [59] Shuai Shao, Zeming Li, Tianyuan Zhang, Chao Peng, Gang Yu, Xiangyu Zhang, Jing Li, and Jian Sun. Objects365: A large-scale, high-quality dataset for object detection. In *ICCV*, pages 8430–8439, 2019. **2, 4, 6, 7, 8**
- [60] Chen Sun, Abhinav Shrivastava, Saurabh Singh, and Abhinav Gupta. Revisiting unreasonable effectiveness of data in deep learning era. In *ICCV*, pages 843–852, 2017. **1, 2**
- [61] Raphael Sznitman and Bruno Jedynak. Active testing for face detection and localization. *TPAMI*, 32(10):1914–1920, 2010. **1, 2**
- [62] Thomas Pellissier Tanon, Gerhard Weikum, and Fabian M. Suchanek. Yago 4: A reason-able knowledge base. *The Semantic Web*, 12123:583 – 596, 2020. **3**
- [63] Bart Thomee, David A Shamma, Gerald Friedland, Benjamin Elizalde, Karl Ni, Douglas Poland, Damian Borth, and Li-Jia Li. Yfcc100m: The new data in multimedia research. *Communications of the ACM*, 59(2):64–73, 2016. **7**
- [64] Simon Tong and Daphne Koller. Support vector machine active learning with applications to text classification. *Journal of machine learning research*, 2(Nov):45–66, 2001. **1, 2**
- [65] Grant Van Horn, Oisin Mac Aodha, Yang Song, Yin Cui, Chen Sun, Alex Shepard, Hartwig Adam, Pietro Perona, and Serge Belongie. The inaturalist species classification and detection dataset. In *CVPR*, pages 8769–8778, 2018. **3, 6**
- [66] Alexander Vezhnevets, Vittorio Ferrari, and Joachim M Buhmann. Weakly supervised structured output learning for semantic segmentation. In *CVPR*, pages 845–852. IEEE, 2012. **1, 2**
- [67] Denny Vrandečić and Markus Krötzsch. Wikidata: a free collaborative knowledgebase. *Communications of the ACM*, 57(10):78–85, 2014. **1, 3**
- [68] Zhirong Wu, Yuanjun Xiong, Stella X Yu, and Dahua Lin. Unsupervised feature learning via non-parametric instance discrimination. In *CVPR*, pages 3733–3742, 2018. **2**

- [69] Jianxiong Xiao, Krista A Ehinger, James Hays, Antonio Torralba, and Aude Oliva. Sun database: Exploring a large collection of scene categories. *IJCV*, 119(1):3–22, 2016. [2](#), [7](#)
- [70] Qizhe Xie, Minh-Thang Luong, Eduard Hovy, and Quoc V Le. Self-training with noisy student improves imagenet classification. In *CVPR*, pages 10687–10698, 2020. [2](#)
- [71] I Zeki Yalniz, Hervé Jégou, Kan Chen, Manohar Paluri, and Dhruv Mahajan. Billion-scale semi-supervised learning for image classification. *arXiv preprint arXiv:1905.00546*, 2019. [1](#), [2](#), [8](#)
- [72] Kaiyu Yang, Klint Qinami, Li Fei-Fei, Jia Deng, and Olga Russakovsky. Towards fairer datasets: Filtering and balancing the distribution of the people subtree in the imagenet hierarchy. In *Proceedings of the 2020 Conference on Fairness, Accountability, and Transparency*, pages 547–558, 2020. [3](#)
- [73] Kaiyu Yang, Jacqueline Yau, Li Fei-Fei, Jia Deng, and Olga Russakovsky. A study of face obfuscation in imagenet. *arXiv preprint arXiv:2103.06191*, 2021. [10](#)
- [74] Linjie Yang, Ping Luo, Chen Change Loy, and Xiaoou Tang. A large-scale car dataset for fine-grained categorization and verification. In *ICCV*, pages 3973–3981, 2015. [6](#)
- [75] Yi Yang, Zhigang Ma, Feiping Nie, Xiaojun Chang, and Alexander G Hauptmann. Multi-class active learning by uncertainty sampling with diversity maximization. *IJCV*, 113(2):113–127, 2015. [1](#), [2](#)
- [76] Sangdoon Yun, Seong Joon Oh, Byeongho Heo, Dongyoon Han, Junsuk Choe, and Sanghyuk Chun. Re-labeling imagenet: from single to multi-labels, from global to localized labels. *arXiv preprint arXiv:2101.05022*, 2021. [5](#)
- [77] Xiaohua Zhai, Joan Puigcerver, Alexander Kolesnikov, Pierre Ruyssen, Carlos Riquelme, Mario Lucic, Josip Djolonga, Andre Susano Pinto, Maxim Neumann, Alexey Dosovitskiy, et al. A large-scale study of representation learning with the visual task adaptation benchmark. *arXiv preprint arXiv:1910.04867*, 2019. [4](#), [6](#)
- [78] Richard Zhang, Phillip Isola, and Alexei A Efros. Colorful image colorization. In *ECCV*, pages 649–666. Springer, 2016. [2](#)
- [79] Shanshan Zhang, Rodrigo Benenson, and Bernt Schiele. Citypersons: A diverse dataset for pedestrian detection. In *CVPR*, July 2017. [2](#), [7](#), [8](#)
- [80] Bolei Zhou, Agata Lapedriza, Aditya Khosla, Aude Oliva, and Antonio Torralba. Places: A 10 million image database for scene recognition. *TPAMI*, 2017. [6](#)
- [81] Barret Zoph, Golnaz Ghiasi, Tsung-Yi Lin, Yin Cui, Hanxiao Liu, Ekin D Cubuk, and Quoc V Le. Rethinking pre-training and self-training. *arXiv preprint arXiv:2006.06882*, 2020. [2](#)
- [82] Ding-Nan Zou, Song-Hai Zhang, Tai-Jiang Mu, and Min Zhang. A new dataset of dog breed images and a benchmark for fine-grained classification. *Computational Visual Media*, 2020. [6](#)